JOURNAL OF BACTERIOLOGY, Mar. 2007, p. 1604–1615 Vol. 189, No. 5
0021-9193/07/$08.00+0 doi:10.1128/JB.00897-06

Oxygen Reactivity of Both Respiratory Oxidases in *Campylobacter jejuni*: the *cydAB* Genes Encode a Cyanide-Resistant, Low-Affinity Oxidase That Is Not of the Cytochrome *bd* Type▽

Rachel J. Jackson,[1]§ Karen T. Elvers,[2] Lucy J. Lee,[1] Mark D. Gidley,[1] Laura M. Wainwright,[1] James Lightfoot,[1] Simon F. Park,[2] and Robert K. Poole[1]*

Department of Molecular Biology and Biotechnology, University of Sheffield, Western Bank, Sheffield S10 2TN, United Kingdom,[1] *and School of Biomedical and Molecular Sciences, University of Surrey, Guildford, Surrey GU2 7XH, United Kingdom*[2]

Received 22 June 2006/Accepted 26 November 2006

The microaerophilic bacterium *Campylobacter jejuni* is a significant food-borne pathogen and is predicted to possess two terminal respiratory oxidases with unknown properties. Inspection of the genome reveals an operon (*cydAB*) apparently encoding a cytochrome *bd*-like oxidase homologous to oxidases in *Escherichia coli* and *Azotobacter vinelandii*. However, *C. jejuni* cells lacked all spectral signals characteristic of the high-spin hemes *b* and *d* of these oxidases. Mutation of the *cydAB* operon of *C. jejuni* did not have a significant effect on growth, but the mutation reduced formate respiration and the viability of cells cultured in 5% oxygen. Since cyanide resistance of respiration was diminished in the mutant, we propose that *C. jejuni* CydAB be renamed CioAB (*c*yanide-*i*nsensitive *o*xidase), as in *Pseudomonas aeruginosa*. We measured the oxygen affinity of each oxidase, using a highly sensitive assay that exploits globin deoxygenation during respiration-catalyzed oxygen uptake. The CioAB-type oxidase exhibited a relatively low affinity for oxygen (K_m = 0.8 μM) and a V_{max} of >20 nmol/mg/s. Expression of *cioAB* was elevated fivefold in cells grown at higher rates of oxygen provision. The alternative, *ccoNOQP*-encoded cyanide-sensitive oxidase, expected to encode a cytochrome *cb′*-type enzyme, plays a major role in the microaerobic respiration of *C. jejuni*, since it appeared to be essential for viability and exhibited a much higher oxygen affinity, with a K_m value of 40 nM and a V_{max} of 6 to 9 nmol/mg/s. Low-temperature photodissociation spectrophotometry revealed that neither oxidase has ligand-binding activity typical of the heme-copper oxidase family. These data are consistent with cytochrome oxidation during photolysis at low temperatures.

Campylobacter jejuni is the predominant bacterial agent of human gastrointestinal infections worldwide and therefore represents a major global public health burden (15). Currently, the development of health protection interventions against this food-borne pathogen is restricted by our limited knowledge of the mechanisms that confer virulence and enable the pathogen to persist within the food chain. The major reservoir for campylobacters is broiler flocks of poultry reared for human consumption. The predominant clinical feature of campylobacteriosis is the development of acute enteritis, abdominal pain, and diarrhea. Uncommon but serious complications may, however, ensue (27). Members of the genus *Campylobacter* are gram-negative, highly motile, flagellate, spirally curved rods. A distinguishing feature is their strictly microaerophilic lifestyle (16), requiring an atmospheric composition of 5 to 10% oxygen and 5 to 13% carbon dioxide for optimal growth, but oxygen metabolism and the basis of microaerophily are poorly understood. Hydrogen and formate are the most effective sources of energy for *C. jejuni* (18). NADH dehydrogenase activity in *C. jejuni* is low, and NADPH acts as a more effective electron donor than NADH in campylobacters (18, 24). The predominant quinone species is dimethylmenaquinone-6 (26). Campylobacters are very rich in *b*- and *c*-type cytochromes, but most of these are uncharacterized. The lack of any spectrophotometric signals in the red spectral region suggests that campylobacters lack cytochromes of the *a* and *d* types (18, 24, 29), but several lines of evidence point to terminally branched respiratory pathways. First, during aerobic formate oxidation, two systems appeared to operate in *Campylobacter sputorum* subsp. *bubulus* (30): one was linked to the respiratory chain and thought to be responsible for proton translocation, and the other was of lower O_2 affinity and tentatively described as a H_2O_2-producing system. Second, cyanide sensitivity studies indicated that the respiratory chain is branched, terminating at two oxidases that differ in their sensitivities to cyanide (18, 24), but the oxidases have not been identified at the molecular level or further characterized.

These early biochemical and physiological studies have been complemented by analysis of the genome sequence of *C. jejuni* NCTC11168, which is predicted to encode components of an aerobic respiratory chain, namely, dehydrogenases (including a putative NADH:quinone reductase, NDH-1), a cytochrome bc_1 complex, and two terminal oxidases (31, 45). Other genes encoding respiratory components include genes for *c*-type cytochromes (Cj0037c, Cj0874c, Cj1020c, Cj1153, Cj1357c, and Cj1358c) and for a putative ubiquinol-cytochrome *c* reductase (Cj1184-6c) (31). Although the existence of cytochrome *o* in succinate-reduced extracts and membranes of *Campylobacter fetus* has been reported (24), the genome sequence does not

* Corresponding author. Mailing address: Department of Molecular Biology and Biotechnology, The University of Sheffield, Western Bank, Sheffield S10 2TN, United Kingdom. Phone: 44-114-222-4447. Fax: 44-114-222-2800. E-mail: r.poole@sheffield.ac.uk.

§ Present address: School of Health and Related Research, The University of Sheffield, Regent Court, Sheffield S1 4DA, United Kingdom.

▽ Published ahead of print on 15 December 2006.

reveal genes likely to encode such an oxidase. The genome also contains genes for two periplasmic cytochrome *c* peroxidases, namely, Cj0020c and Cj0358 (31). Genes annotated as encoding a "cytochrome *bd* oxidase" are present (Cj0081-2), in addition to genes coding for a putative "*cb*-type cytochrome *c* oxidase" or "cytochrome cbb_3-type oxidase" (Cj1487c, Cj1488c, Cj1489c, and Cj1490c) (31, 45).

In this paper, we describe a detailed study of the oxygen reactivity of *C. jejuni* and assign distinct oxygen affinities and cyanide sensitivities to the two oxidases. Such studies contribute to an understanding of the microaerophilic lifestyle of this important human pathogen.

MATERIALS AND METHODS

Bacterial strains. The wild-type strain used was *C. jejuni* strain NCTC11168. A mutant strain defective in *cydAB* was constructed as follows. Genomic DNA was isolated from *C. jejuni* as described before (32). The *cydA* (Cj0081) and *cydB* (Cj0082) genes were amplified by PCR, using the oligonucleotide primers CYD1 (5′-AACTCTTGGAAAGACCCTTTGGAAA-3′) and CYD2 (5′-GGATCCAA TTACTAAAGGCCAAGCCAATAA-3′). The 2,904-bp DNA fragment was cloned into the pBAD-TOPO TA cloning vector (Invitrogen) and oriented using BamHI (restriction site is underlined). Inverse PCR (54) was performed using the primers CYD3 (5′-GCAACAAGATCTAGTCCTGCACGATGTTCACCT TGAT-3′) and CYD4 (5′-GCAACAAGATCTTCGATGAGCTTAGCAAGGA TGAGCT-3′), resulting in the deletion of 866 bp, mostly from *cydA*, and introducing a unique BglII restriction site (underlined). The PCR product was digested using BglII and self-ligated before transformation into *Escherichia coli* DH5α cells. Plasmid DNA was recovered and digested with BglII. A kanamycin resistance cassette was excised from pJMK30 (48) by digestion using BamHI. This kanamycin resistance cassette was ligated into the plasmid construct, thereby inactivating *cydAB* by insertion into the operon. The resulting construct was introduced into competent *C. jejuni* cells by electroporation. Integration into the chromosome occurred via double homologous recombination. Transformants were selected on Mueller-Hinton agar containing kanamycin at 50 μg/ml and confirmed as defective in *cydAB* by PCR and Southern blot analysis. This strain is referred to as RKP1341.

Media and culture conditions. Cells were maintained at −70°C as stocks containing 15% (vol/vol) glycerol and 3.7% (wt/vol) brain heart infusion broth. Cells were streaked onto Mueller-Hinton agar (Oxoid) and incubated for 48 h at 37°C in a sealed jar containing a microaerobic atmosphere generated by a CampyGen sachet (Oxoid). Cells from plates were inoculated into 50 ml Mueller-Hinton broth (Oxoid) in 100-ml flasks and shaken overnight at approximately 115 rpm in a modular atmosphere-controlled system VA500 workstation (Don Whitley Scientific) maintained at 42°C with a constant gas supply of 10% oxygen, 10% carbon dioxide, and 80% nitrogen (unless specified otherwise). Wild-type cells were grown in the presence of amphotericin B and vancomycin HCl (Duchefa) at 10 μg/ml. Cultures of the *cydAB* mutant also contained kanamycin at 50 μg/ml for selection. After approximately 18 h, starter cultures were used to give a 3% (vol/vol) inoculation of 150 ml of Mueller-Hinton broth in 250-ml-capacity baffled flasks (Bellco). These cultures were incubated microaerobically in the VA500 workstation with constant shaking. For batch growth, cultures were typically harvested at an optical density at 600 nm (OD_{600}) of 0.2 (after shaking for approximately 8 h), and cells were washed twice in 50 mM potassium phosphate buffer (pH 7.3) and either used immediately or stored at −20°C. Viable counts were performed by serially diluting portions of microaerobically grown cells in 50 mM potassium phosphate buffer (pH 7.3) under atmospheric conditions, plating them on Mueller-Hinton agar, and microaerobically incubating them in the modular atmosphere-controlled system workstation.

Real-time PCR. *C. jejuni* NCTC11168 broth cultures in Mueller-Hinton broth (100 ml and 200 ml) were incubated in 250-ml flasks, and the total volumes were harvested directly into 6.3 ml prechilled phenol (made up in 118.7 ml 100% ethanol) to stabilize the RNA. Samples were centrifuged at 5,500 rpm for 4 min (4°C), and total RNA was purified from cell pellets, using a QIAGEN RNeasy Mini kit as recommended by the supplier. RNA concentration and purity were determined by A_{260}/A_{280} measurements. cDNA synthesis was carried out using 4 μg of starting material primed with 9 μg poly$(dN)_6$ random hexamers (Amersham Biosciences). Reaction mixes (20 μl) containing 0.5 mM (each) dATP, dTTP, dGTP, and dCTP were incubated for 2 h at 42°C with 200 units Superscript II RNase H reverse transcriptase (Invitrogen). Following synthesis, cDNA was purified using a PCR purification kit (QIAGEN) to remove unincorporated deoxynucleoside triphosphates and primers. Gene-specific primers were designed to amplify 50- to 150-nucleotide fragments of target genes, using PRIMER 3 software (42). Sequences for the primers are as follows: *gyrA* (internal control) forward, 5′-ATGCTCTTTGCAGTAACCAAAAAA-3′; *gyrA* reverse, 5′-GGCCGATTTCACGCACTTTA-3′; *cydA* forward, 5′-CGAACTTAG TAGCGTTGATTGG-3′; *cydA* reverse, 5′-CAAGCCTAAGGTTAAAGGCAC A-3′; *cydB* forward, 5′-TTGCTGTTTTGCTTGTTATTGG-3′; and *cydB* reverse, 5′-CTGTTAAAACCGTTCCAAGTCC-3′. A SYBR green mix was made at a ratio of 13 μl Quantace Sensimix (Bioline), 0.5 μl SYBR green, and 4.5 μl nuclease-free water (Sigma). Each reaction was carried out in a total volume of 25 μl in a 96-well optical reaction plate (Applied Biosystems). Each well contained 16 μl SYBR green mix (above), 12.5 pmol of each of the two primers, and 5 μl of cDNA sample. PCR amplification was carried out in an ABI 7700 thermocycler (PE Applied Biosystems), with the following thermal cycling conditions: 50°C for 2 min and 95°C for 10 min, followed by 40 cycles of 95°C for 15 s and 60°C for 1 min. Data were analyzed using the manufacturer's Sequence Detector system software and further processed in Microsoft Excel. A standard curve was established using genomic DNA for each gene studied to confirm that the primers amplified at the same rate. The relative levels of expression of genes of interest in 200-ml cultures compared with those in 100-ml cultures were calculated following a protocol for the standard curve method (1a). No-template reactions were included as negative controls.

Preparation of soluble and membrane fractions. The methods for preparation of soluble and membrane fractions were based on earlier protocols (18, 34). Whole cells were resuspended in 50 mM potassium phosphate buffer (pH 7.3) at 4°C and sonicated (six cycles of 15 s each) in a Sanyo Soniprep 150 instrument. The sonicate was then spun for 15 min at 12,000 × *g*. The supernatant was retained and spun for 60 min at 55,000 rpm (207,000 × *g*). The soluble fraction was retained. The membrane pellet was gently resuspended in a small volume of 50 mM potassium phosphate buffer. Protein concentrations were determined by the method of Markwell et al. (25). All fractions were stored at −70°C.

Measurement of oxygen consumption using a Clark-type electrode. A digital Clark-type electrode system (model 10; Rank Brothers, Bottisham, Cambridge, United Kingdom) was used to measure oxygen consumption. The electrode was calibrated by using air-saturated 50 mM potassium phosphate buffer (pH 7.3), assuming an oxygen concentration of 220 μM, and sodium dithionite to zero the electrode. The buffer was then air saturated by stirring for 10 min, and after capping of the chamber, additions were made using Hamilton microliter syringes through a capillary hole. The effect of NaCN on respiratory activity was tested by adding a freshly prepared solution to a final concentration of 100 or 125 μM approximately 5 min before adding sodium formate (5 mM final concentration).

Room temperature spectrophotometry. Electronic absorption spectra were measured using a custom-built SDB4 dual-wavelength scanning spectrophotometer (University of Pennsylvania School of Medicine Biomedical Instrumentation Group and Current Designs, Philadelphia, PA) (21). Harvested cells were washed and resuspended in 50 mM potassium phosphate buffer (pH 7.3) for spectroscopy (dithionite-reduced minus air-oxidized and reduced-plus-CO minus reduced difference spectra). Cytochrome concentrations were calculated using the following extinction coefficients: cytochrome *c*, 19.1 mM^{-1} cm^{-1} (α peak minus α trough) (4); cytochrome *b*, 17.5 mM^{-1} cm^{-1} (560-nm value minus 575-nm value) (20); and CO-binding cytochrome *c*, 25 mM^{-1} cm^{-1} (α peak minus α trough) (52).

Photodissociation spectrophotometry at subzero temperatures. Low-temperature spectral work was based on earlier work (37). Intact cells from liquid cultures grown at 10% oxygen or subcellular fractions were supplemented with ethylene glycol (final concentration, 30% [vol/vol]) and reduced with a few grains of sodium dithionite. CO was introduced as described for the room-temperature studies; all further manipulations were performed in the dark to prevent photodissociation of the CO complex until its activation by actinic light. The cuvette was cooled to −78°C in an ethanol-solid CO_2 bath for 10 min, transferred to the sample compartment of the dual-wavelength spectrophotometer, and equilibrated at the experimental temperature. The temperature was controlled by a flow of nitrogen gas, cooled by passage through a coiled copper tube immersed in liquid nitrogen and then through a small heater. Photolysis was achieved with a focused beam of actinic white light from a 150-W slide projector. Following 5 min of illumination, difference spectra (postphotolysis minus prephotolysis) were recorded immediately and every 5 min thereafter for 30 min. All spectra shown are typical of duplicate or triplicate experiments for each condition studied.

Determination of oxygen affinities. Leghemoglobin from soybean nodules and myoglobin (from ferric horse skeletal muscle; Sigma) were converted to the oxy forms (9). In brief, 2 mM solutions in 25 mM potassium phosphate buffer plus 1 mM EDTA (in MilliQ water) were reduced by adding sodium dithionite (0.1 M),

prepared in 10 mM NaOH, and sparged for 15 min with nitrogen gas at a concentration of 2.5 times that of the globin. A Pharmacia Biotech Sephadex G-25 M PD-10 column was equilibrated with air-saturated buffer (5 to 10 times the column bed volume), with nitrogen gas blowing over the surface, and buffer was allowed to run down to the level of the PD-10 sinter. The ferrous myoglobin solution was then added under nitrogen and allowed to reach the sinter level. The headspace of the column was filled with buffer, and the eluate was collected. The absolute spectrum of the eluate was scanned against a buffer baseline to confirm the identity of the eluate as oxymyoglobin. Oxyglobins were stored at −70°C.

Oxygen affinity studies were performed essentially as described before (9), using the dual-wavelength scanning spectrophotometer, but in time-scanning mode. Oxyleghemoglobin and oxymyoglobin solutions were diluted in the buffer described above and deoxygenated by being sparged with nitrogen gas at final concentrations of 15 μM and 10 μM, respectively. A purpose-built glass cuvette with a 1-cm path length and approximately 1.5-ml capacity was fitted with a Subaseal with glass capillary tubing inserted through it. Solutions were added to the cuvette via the glass tubing, using a Hamilton syringe. A small magnetic stirrer bar in the cuvette continuously mixed the contents; electromagnetic interference was avoided by μ shielding the photomultiplier. The cuvette was completely filled with a solution of oxyglobin (approximately 15 μM), and approximately 30 s later, a suspension of cells grown at 10% oxygen or derived membranes were added to give a total protein content (ω) of approximately 0.5 mg. After 30 s, sodium formate (final concentration, 5 mM) was added to initiate respiration. Sodium dithionite (final concentration, 2 mM) was added at the end to ensure that deoxygenation had occurred. Spectral and absorbance-time data were stored in an iMac computer and analyzed using SoftSDB (Current Designs). The rate of oxygen consumption, V, and the average concentration of free dissolved oxygen, S, were calculated using Microsoft Excel software. For leghemoglobin, ΔA (576 nm minus 565 nm) was measured, while for myoglobin, ΔA (582 nm minus 565 nm) was monitored. For soybean leghemoglobin, $K' = 43.5 \times 10^{-9}$ M; for horse skeletal muscle myoglobin, $K' = 786 \times 10^{-9}$ M. Data obtained where Y_t was <0.1 were not used in order to avoid possible errors caused by the generation of ferric globin by autoxidation (3), and only data with Y_t values that fell between 0.85 and 0.15 were analyzed, as these points were well within the reliable working range of the globins used. Plots of $1/V$ against $1/S$ (Lineweaver-Burk) and V against V/S (Eadie-Hofstee) were calculated. Eadie-Hofstee plots were taken to be the more reliable linear transformation (11). K_m values were determined using the linear regression feature of the software, and V_{max} values were estimated using plots of V against S or Lineweaver-Burk plots.

Formaldehyde assays. Formaldehyde assays were based on published methods (2). CO was slowly bubbled through dithionite-reduced whole cells or membrane suspensions for 10 min. The cuvette contents were exposed to actinic white light for 15 min, and the cuvette contents were then decanted and kept on ice. Samples (0.5 ml) were taken at 15- and 30-min intervals and mixed with 0.75 ml trichloroacetic acid. Tubes were spun at 38,100 × *g* to pellet cell debris, and the supernatant fraction (1 ml) was mixed with 0.5 ml Nash reagent. Tubes were incubated at 60°C for 10 min, and the production of 3,5-diacetyl 1,4-dihydrolutinin was quantified by measuring the absorbance at 412 nm. Formaldehyde concentrations were quantified using a calibration curve.

RESULTS

Growth properties of a *cydAB* mutant. Optical densities were measured for wild-type and *cydAB* mutant strains growing in atmospheres containing either 5% or 10% (vol/vol) oxygen (Fig. 1). For both strains, the mean doubling time was approximately 5 h, as determined from the period of exponential growth. Wild-type and *cydAB* strains grown at 5% oxygen (Fig. 1A) showed slightly but consistently higher final cell densities than those cultured at 10% oxygen (Fig. 1B) (OD, 0.55 and <0.50, respectively). Cultures of wild-type and *cydAB* strains at 10% (vol/vol) oxygen showed slight decreases in density during the later stages of growth. After 12 h, wild-type cultures incubated at 5% oxygen showed much higher viabilities—over 1.6×10^9 CFU/ml (Fig. 1A)—than did cultures of the *cydAB* mutant strain, at approximately 7×10^8 CFU/ml. The cell viabilities of wild-type and *cydAB* strains grown at 10% oxygen were roughly equivalent, at approximately 8×10^8 to 9×10^8

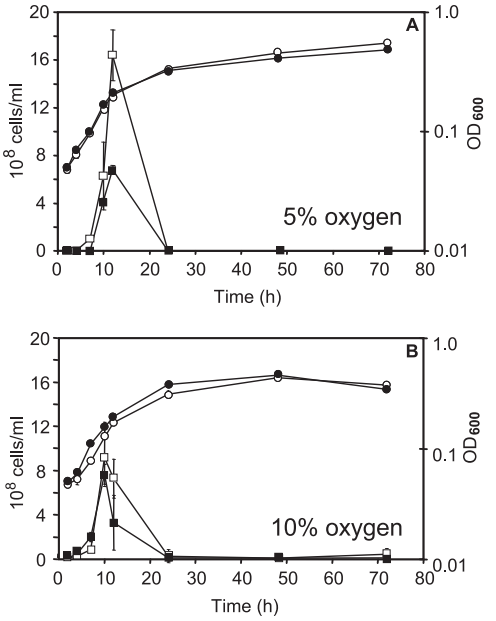

FIG. 1. Cell viabilities and OD_{600} values (apparent absorbance at 600 nm) over time for wild-type (RKP4818) and *cydAB* mutant (RKP1341) liquid batch cultures of *C. jejuni*. Panel A shows data for cells grown at 5% (vol/vol) oxygen, and panel B shows data for cells grown at 10% (vol/vol) oxygen. Viability data are shown as squares, and OD values are shown as circles; the wild-type strain is represented by open symbols, and the *cydAB* mutant is represented by closed symbols. All points represent the mean values calculated for duplicate experiments. Standard deviations are shown as bars for each point but are often within the size of the data points.

CFU/ml. Despite the small numbers of viable cells recovered from microaerobically grown cultures (after dilution under atmospheric conditions), these results indicate a viability deficiency of the *cydAB* mutant relative to the wild-type strain at 5% O_2. The increasing optical densities of these cultures, yet sharp decline in viability at the end of exponential phase, are attributed in part to the transition of rod-shaped cells into the degenerate coccoid form during the late stages of culture (22). Although a precipitous decline in culture viability was observed in triplicate experiments, we considered verifying the higher viability of wild-type cells by competitive coculture of the two strains. However, there is a remote possibility of transfer of the kanamycin resistance cassette between mutant and wild-type cells, since *C. jejuni* is naturally competent.

It is most unlikely that insertion into *cydAB* of the kanamycin resistance cassette would introduce polar effects on downstream genes. Genes downstream of *cydAB* (Cj0085c and Cj0086c) are on the opposite DNA strand and are unlikely to be affected. Furthermore, they encode proteins (an amino acid racemase and a uracil-DNA glycosylase) that are unlikely to be involved in the phenotypic changes studied here. The kanamycin resistance cassette used bears its own promoter but lacks a transcriptional terminator, and when this cassette is inserted (as described here) with the same transcriptional polarity as the mutated gene, the resulting mutations have been shown to be nonpolar on downstream genes (17). Nevertheless, we attempted to complement the *cydAB* mutation, which spans *cydA* and *cydB*, while recognizing the difficulty of using a comple-

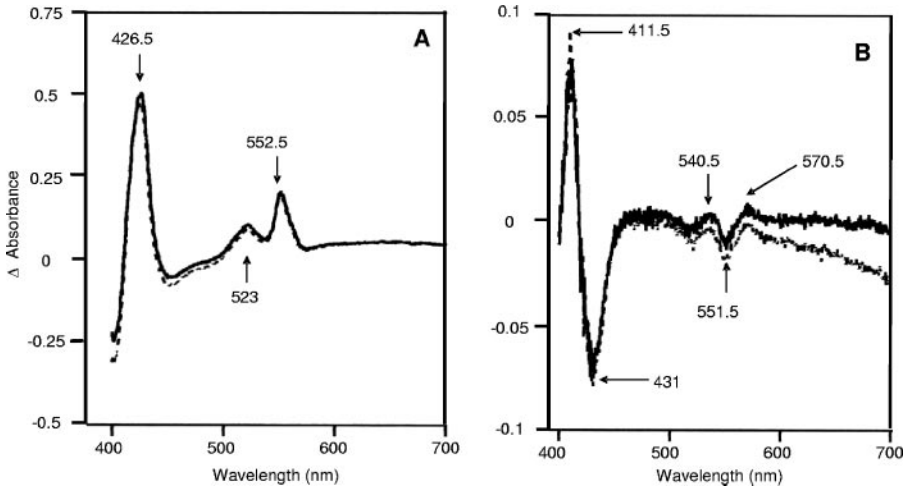

FIG. 2. Room-temperature spectrophotometric analysis of wild-type and *cydAB* strains. (A) Reduced minus oxidized difference spectra for wild-type (solid lines) and *cydAB* (dashed lines) cells grown at 10% (vol/vol) oxygen. (B) Corresponding CO difference spectra. The protein concentration was 3.0 mg/ml throughout.

menting fragment (*cydA* plus *cydB*) that is large relative to the region that mediates recombination. The general approach for complementation has been described before (14). A 3,210-bp fragment comprising *cydAB* was cloned into pGEMCWH01 to generate the suicide plasmid pKE123, comprising a wild-type copy of *cydAB* and, downstream, a selectable chloramphenicol marker flanked by Cj0752 (the insertion site for complementation). This was introduced into competent cells of RKP1341 by electroporation, and transformants were selected on Mueller-Hinton agar with chloramphenicol (10 μg ml^{-1}). In all chloramphenicol-resistant transformants obtained in three attempts, the vector was integrated into the original *cydAB* locus, not at the second site needed for complementation.

Cytochrome composition of the respiratory chain. Gross changes in cytochrome profile were sought using reduced-minus-oxidized difference spectra at room temperature for wild-type and *cydAB* whole cells grown at 5 or 10% oxygen. These are shown in Fig. 2A for 10% oxygen and are qualitatively similar. Peaks were present at 426.5, 523, and 552.5 nm (Soret, β, and α, respectively). Surprisingly, in view of the presence of a *cydAB*-like operon in the *C. jejuni* genome, there were no spectral features attributable to a cytochrome *bd*-type oxidase, i.e., peaks at about 630 nm (cytochrome *d*) and 595 nm (high-spin heme *b*) were absent. Figure 2B shows the CO difference spectra for wild-type and *cydAB* whole cells grown at 10% oxygen, which exhibit very similar features and signal sizes. Peaks were observed at 411.5, 540.5, and 570.5 nm, while troughs were located at 431 and 551.5 nm. Importantly, the distinctive features of a cytochrome *bd*-type oxidase (Soret signals of >440 nm and α-absorbance in the 630- to 640-nm region) were again absent in both wild-type and mutant cells.

The amounts of cytochromes present in wild-type and *cydAB* cultures incubated at 5% and 10% oxygen were quantified (Table 1). Despite uncertainty in ascribing signal intensities to the overlapping absorbances of cytochromes *b* (λ_{max}, 560 nm) and *c* (λ_{max}, 552.5 nm), there were no major differences in cytochrome levels observed between strains under either growth condition. However, cells grown at 10% oxygen contained higher concentrations of cytochromes *c* and *b* and CO-binding hemoproteins than did cultures incubated at 5% oxygen. Thus, oxygen tension influences the levels of cytochromes in *C. jejuni* cells in mid- to late exponential growth, but the consequences of *cydAB* mutation were not evident by room-temperature difference spectroscopy.

TABLE 1. Cytochrome contents and respiratory activities of wild-type (RKP4818) and *cydAB* (RKP1341) strains of *C. jejuni*

Growth condition	Strain	Cytochrome content (nmol cytochrome/mg protein)[a]			Initial formate-supported respiratory rate (nmol O_2 consumed/s/mg of protein[a]		% Inhibition by cyanide
		Cytochrome *c*[b]	Cytochrome *b*[b]	CO-binding cytochrome *c*[c]	Without cyanide	With 125 μM NaCN[d]	
5 % oxygen	Wild type	1.51 (0.035)	0.98 (0.049)	0.14 (0.006)	21.5 (1.22)	5.33 (0.57)	75
	cydAB mutant (Cio^-)	1.56 (0.061)	0.93 (0.070)	0.16 (0.032)	14.6 (2.10)	4.18 (0.17)	71
10 % oxygen	Wild type	2.50 (0.031)	1.69 (0.017)	0.27 (0.032)	20.8 (1.24)	12.1 (0.62)	42
	cydAB mutant (Cio^-)	2.49 (0.025)	1.65 (0.053)	0.27 (0.006)	14.8 (0.85)	4.05 (0.57)	73

[a] The results shown are mean values for experiments performed in triplicate or quadruplicate in which the maximum deviation from the means shown was 20%. Standard deviations are shown in parentheses.
[b] Determined from reduced minus oxidized difference spectra.
[c] Determined from reduced-plus-CO minus reduced difference spectra.
[d] NaCN was preincubated with cells for 5 min before the addition of formate.

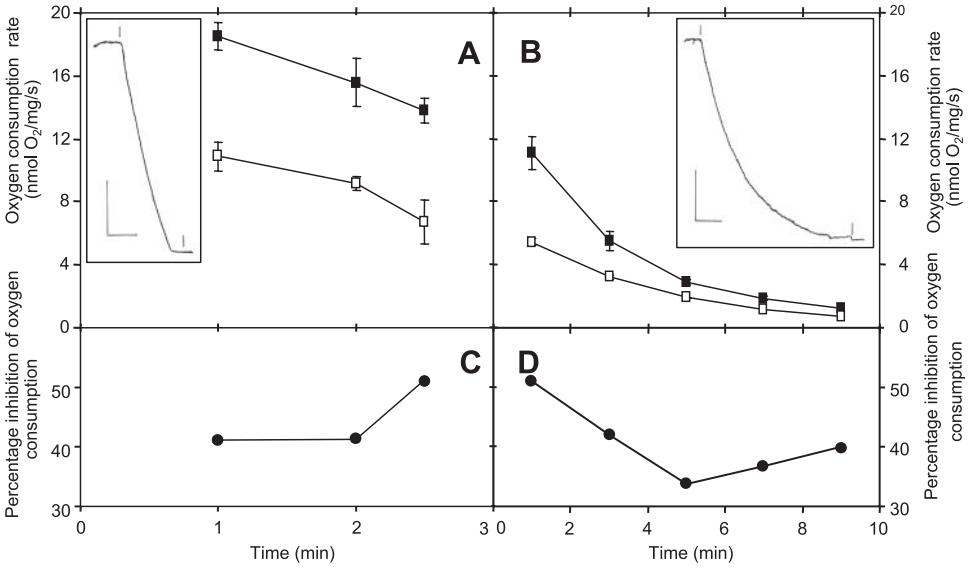

FIG. 3. Respiration of *C. jejuni* and effects of cyanide on wild-type and *cydAB* whole cells. Respiration rates are plotted as a function of time after the addition of formate to resting cell suspensions for both wild-type (A) and *cydAB* mutant (B) cells. The insets show typical oxygen electrode traces over the period leading to oxygen depletion in the chamber. In the insets, the vertical bars represent 20% air saturation (approximately 40 μM O_2), and the horizontal bars represent 2 min. At the first marker, formate was added, and at the second, sodium dithionite was added. In main panels A and B, respiration rates were plotted for the absence (closed symbols) and presence (open symbols) of 100 μM cyanide, which was added 5 min before formate. The percentage of inhibition by cyanide is shown for wild-type (C) and *cydAB* mutant (D) cells.

To investigate cytochrome levels in older cultures, wild-type and *cydAB* cells were also incubated microaerobically at 37°C and harvested after 48 h of growth on Mueller-Hinton agar. The amounts of cytochromes present in these older cultures were quantified (data not shown) after subcellular fractionation. The *cydAB* mutant was consistently deficient in soluble cytochrome *c* and membrane-bound cytochrome *b* after 48 h of growth under microaerobic conditions. Cytochrome *c* was present in the high-speed supernatant fraction of wild-type cells at 1.1 nmol/mg of total protein, compared to approximately 0.7 nmol/mg for a *cydAB* fraction. Levels of membrane-bound cytochrome *b* were also halved, from about 0.2 to 0.1 nmol/mg of total protein in wild-type and *cydAB* membrane fractions, respectively.

In an attempt to express the CydAB-like oxidase in *E. coli* and to characterize the heme content in an oxidase-deficient background, we introduced a plasmid bearing wild-type *cydAB*$^+$ (see Materials and Methods) into an *E. coli cydAB* mutant. However, the transformed cells showed very poor growth and were unsuitable for biochemical characterization.

Respiratory activities reveal a *cydAB* phenotype. To evaluate the functional consequences of *cydAB* mutation, wild-type and *cydAB* cultures were grown to late exponential phase in atmospheres containing 5% and 10% oxygen, and oxygen consumption rates were measured using an oxygen electrode. Wild-type cells grown at 5% or 10% oxygen tension displayed similar initial oxygen uptake rates of >20 nmol oxygen consumed/s/mg of total protein (Table 1). Whole cells of *cydAB* mutant cultures, however, grown at both 5% and 10% oxygen levels possessed consistently lower initial respiratory rates (<15 nmol O_2/s/mg of total protein) (Table 1). These values for the *cydAB* mutant are higher than the values calculated for the V_{max} of the highest-affinity oxidase (see below) and might therefore include contributions to oxygen uptake by systems, perhaps soluble, of very low oxygen affinity, which would not have been detectable in the globin-based assays (see below). Thus, irrespective of the oxygen concentration in the growth atmosphere, the initial rates of respiration of *cydAB* mutant cells were lower than the wild-type rates.

To assess the cyanide resistance of the *cydAB*-encoded oxidase, initial formate-supported respiration rates were measured polarographically for cells (grown with 10% oxygen) preincubated in the electrode chamber with 100 μM sodium cyanide. The polarographic traces for the wild-type strain exhibited a rapid oxygen uptake that was maintained for several minutes (see inset in Fig. 3A), with the rate declining by ca. 20% as oxygen was consumed (Fig. 3A). In the presence of cyanide, there was an almost parallel decline in the oxygen consumption rate with time (Fig. 3A), such that the percentage of inhibition of respiration by cyanide was uniform, at 40%, over 2 min, rising to 50% as the oxygen tension in the chamber approached zero, at 2.5 min (Fig. 3C). In marked contrast, respiration of the *cydAB* mutant was markedly nonlinear (see inset in Fig. 3B), declining by 50% over 2 min, and the initial formate-supported oxygen uptake rate was only 60% (Fig. 3B) of that for the wild-type strain (Fig. 3A). In the presence of 100 μM sodium cyanide, a declining rate of oxygen uptake was again observed, and the calculated percentage of inhibition was higher, at >50% at early time points, declining as oxygen was consumed (Fig. 3D).

To quantify the inhibition by cyanide of cells grown under different conditions, the cyanide concentration for preincubation of the cells was raised to 125 μM sodium cyanide, and the inhibition of respiration was measured during the first 2 min after formate stimulation in order to observe maximal inhibition (Fig. 3C and D). Table 1 shows the respiratory activities of

wild-type and *cydAB* whole cells grown at 5% and 10% oxygen. Wild-type cells cultured at 10% oxygen displayed the highest cyanide-insensitive oxygen uptake rates (>12 nmol/s/mg), representing 42% inhibition of respiration. However, wild-type cells grown at only 5% oxygen displayed significantly lower rates of oxygen consumption in the presence of cyanide (>5 nmol/s/mg), representing a 75% inhibition of respiration. In contrast, the *cydAB* mutant was sensitive to 125 μM cyanide when cultured at both 5% and 10% oxygen, showing a decreased respiratory rate, of approximately 4.1 nmol oxygen consumed/s/mg, under both oxygen tensions. Thus, *cydAB* mutant cells exhibit a clear phenotype, namely, markedly nonlinear O_2 uptake (Fig. 3B), decreased oxygen uptake rates, and a markedly increased sensitivity to cyanide when grown at 10% oxygen (Fig. 3; Table 1).

To investigate further the relationship between oxygen, expression of CydAB, and cyanide insensitivity, the oxygen transfer rate to cultures was systematically varied by using 100, 150, or 200 ml of medium in 250-ml baffled flasks. The first-order rate constant (*K*) for oxygen diffusion into the medium from the microaerobic atmosphere (33) was determined for each volume and found to be 0.43, 0.16, and 0.06 min^{-1}, respectively. Direct evidence for increased expression of *cydAB* with elevated oxygen availability was obtained by quantification of *cydA* and *cydB* transcripts by reverse transcription-PCR (RT-PCR). Cells were grown at *K* values of 0.43 and 0.06 min^{-1} and used for RNA extraction and RT-PCR. For both *cydA* and *cydB*, triplicate assays showed a 5.0-fold increase in transcript abundance at the higher O_2 transfer rate. Further evidence for expression of the *cydAB* genes in laboratory cultures was obtained in microarray experiments (see Discussion). Exponentially growing cells from each condition were also used to measure formate-supported respiration rates in both the absence and presence of 125 μM KCN. With decreasing oxygen diffusion, the percentage of respiration that was uninhibited by cyanide also decreased, by the following amounts (each measurement is the mean of three separate determinations): 53.9% ($K = 0.43\ min^{-1}$), 47.1% ($K = 0.16\ min^{-1}$), and 39.4% ($K = 0.06\ min^{-1}$). Thus, wild-type cells exhibit increasingly cyanide-resistant respiration when cultured at higher oxygen availability, which we attribute to the *cydAB*-encoded oxidase because of its lower affinity for oxygen (see below).

The lack of distinctive spectral signals for the CydAB-like oxidase (Fig. 2) precluded quantitation against the background of other *c*- and *b*-type cytochromes. We therefore attempted an immunological assay using an antibody directed against the *Pseudomonas aeruginosa* CioA protein (5), but it was nonspecific and failed to detect bands of the anticipated sizes. We therefore designed and synthesized a peptide representing the putative Q loop (12) of *C. jejuni* CydAB, namely, NH_2-Cys-Ile-Leu-Asn-Pro-Lys-Lys-Thr-Ile-Asp-Asn-Asn-Glu-Ser-Val-Phe-COOH. Antibodies were raised to this peptide as described before (46), but again, nonspecific binding prevented oxidase identification and quantitation in gels containing cell extracts.

Is there an essential role for the *cco*-encoded oxidase? Attempts were made to construct a mutant strain of *C. jejuni* which is deficient in the cytochrome *cb′*-type oxidase, presumed to be encoded by *ccoP* (Cj1487c), *ccoQ* (Cj1488c), *ccoO* (Cj1489c), and *ccoN* (Cj1490c). A region spanning *ccoO* and *ccoN* was amplified by PCR, and a kanamycin resistance cassette was inserted. However, after electroporation, no transformants were obtained, despite repeated attempts.

Determination of the oxygen affinities of the two terminal oxidases of *C. jejuni* cells, using deoxygenation of oxyleghemoglobin and oxymyoglobin. Early studies of formate oxidation by *C. sputorum* subsp. *bubulus*, using an oxygen electrode, reported two oxidase components with K_m values of about 4 μM and 1 mM (30), but polarography is not suited to the determination of high affinities. The globin-based technique used here has revealed very-high-affinity oxidases in several studies (8, 10).

The visible absorption spectrum of soybean oxyleghemoglobin possesses maxima in the α and β regions at 540 and 575 nm, whereas the deoxygenated or reduced form is characterized by a single peak at 557 nm. Similarly, the spectrum of horse skeletal muscle oxymyoglobin possesses maxima at 544 nm and 582 nm, whereas the deoxygenated form shows a single peak at 558 nm (for these spectra, see reference 9). Therefore, for leghemoglobin, the absorbance change between 575 nm and 560 nm (an isosbestic point) was measured in dual-wavelength mode to follow conversion from the oxy- to the deoxyform as a result of bacterial oxygen consumption. Deoxygenation of oxymyoglobin was monitored at 565 nm to 582 nm (an isosbestic point). The rates of respiration of *C. jejuni* whole cells at low oxygen concentrations were measured by monitoring, in separate experiments, the deoxygenation of oxyleghemoglobin (range, 0.003 to 0.3 μM O_2) and oxymyoglobin (range, 0.3 to 10 μM O_2).

The addition of cells to nitrogen-sparged buffer containing oxyleghemoglobin resulted in an instantaneous drop in absorbance, which was attributed to an optical rather than biological effect (Fig. 4A, letter "b"). Absorbance was stable while the cells respired, using the small amount of oxygen present in the buffer. When the buffer became oxygen depleted, the globin underwent deoxygenation as the cells continued to respire, observed as a decrease in ΔA (Fig. 4A, letter "c"). Deoxygenation of oxyleghemoglobin by wild-type cells allowed calculation of the total dissolved oxygen concentration with time (Fig. 4B). The Eadie-Hofstee plot of these data (Fig. 4C, closed squares) clearly reveals a single component with a K_m value of 40 nM. V_{max} was found to be 5.4 nmol/mg/s. Similar experiments with leghemoglobin as the oxygen donor for the formate-supported respiration of *cydAB* mutant cells (Fig. 4C, open squares) again showed a single high-affinity component with a K_m value of 42 nM (apparent V_{max}, 8.93 nmol/mg/s). The presence of this high-affinity component in both wild-type and *cydAB* whole cells allowed us to unambiguously assign its activity to the *cb′*-type cytochrome *c* oxidase.

Experiments with oxymyoglobin as the oxygen source were also performed to study oxidases of lower affinity. Figure 5 shows the declining oxygen concentration with time for wild-type (closed squares) and mutant (open squares) cells. In the case of wild-type cells, the oxygen concentration fell linearly until it reached approximately 5 nM. Only at lower oxygen concentrations did the rate of respiration decline as oxygen was consumed (i.e., the oxygen-time plot in Fig. 5 became nonlinear), so only the last 15 time points spanning this region of oxygen dependence were analyzed further. The resulting Eadie-Hofstee plot (not shown) followed a monophasic pattern, revealing a single low-affinity component with a K_m value

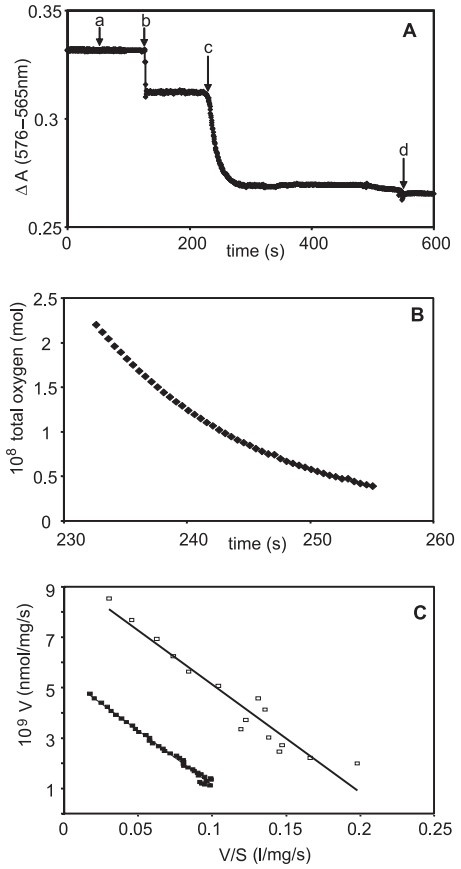

FIG. 4. Deoxygenation of oxyleghemoglobin by *C. jejuni* whole cells and determination of reactivity of the high-affinity oxidase. Panel A shows the deoxygenation of oxyleghemoglobin by wild-type whole cells. At time zero, the cuvette contained 17 μM oxyleghemoglobin in buffer, previously sparged with nitrogen. Formate (5 mM) was added (a), followed by whole cells (ω = 0.35 mg) (b), whose turbidity produced a downward deflection in ΔA. Between times b and c, cells consumed free oxygen in solution, but this did not cause deoxygenation of the globin. At time c, after near exhaustion of free oxygen, spontaneous deoxygenation of the globin occurred. Excess sodium dithionite was added to complete deoxygenation (d). Panel B shows total oxygen against time in the presence of leghemoglobin and wild-type cells; note that the timescale includes only that part of the deoxygenation trace (A) that reveals globin deoxygenation. Panel C shows Eadie-Hofstee plots for deoxygenation of oxyleghemoglobin by wild-type (closed squares) and *cydAB* (open squares) whole cells.

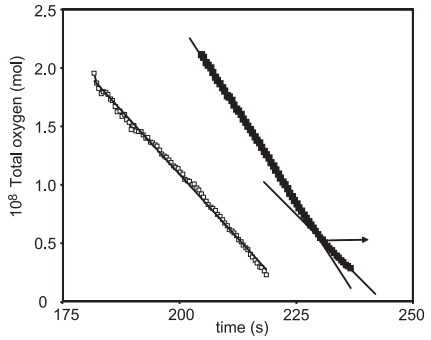

FIG. 5. Deoxygenation of oxymyoglobin by *C. jejuni* cells and determination of reactivity of the low-affinity oxidase. Total oxygen was plotted against time in the presence of *cydAB* (open squares) or wild-type (closed squares) cells. Notice the presence of a low-affinity component (final 15 data points) in the wild-type experiment only; these were smoothed according to the line of best fit ($y = 71.679e^{-0.1012}x$; $R^2 = 0.9973$) (not shown) and analyzed using an Eadie-Hofstee plot (see text).

of 0.83 μM and a V_{max} of 20 nmol/mg/s. In the case of the *cydAB* mutant (open symbols in Fig. 5), the oxygen concentration declined linearly with time, and no oxygen-dependent phase at low oxygen concentrations was observed. There was therefore no evidence in *cydAB* mutant cells for a component with an oxygen affinity in the range covered by myoglobin (0.3 to 10 μM), and we attribute the low-affinity activity in wild-type cells to the CydAB-type oxidase. Table 2 summarizes the K_m and V_{max} values for *C. jejuni* wild-type and *cydAB* whole cells calculated from the deoxygenation of oxyleghemoglobin and oxymyoglobin.

Analysis of the respiratory activities of *C. jejuni* membrane fractions. Membranes were capable of only partially deoxygenating oxyleghemoglobin, and it was not possible to produce full deoxygenation curves for data analysis. The formate-supported respiration of membranes measured in an O_2 electrode is shown in Fig. 6. Figure 6A and C show measurements of the respiratory activity of wild-type membranes, while corresponding measurements made using *cydAB* membranes are shown in panels B and D. At the start of each trace, membranes in buffer were supplemented with formate (final concentration, 5 mM) at the time marked by arrow b on each trace. In each panel, at the time marked by arrow c, excess dithionite was added to show the extent of reduction of oxygen achieved in each case. Wild-type membranes exhibited a mean oxygen consumption rate of 5.7 nmol/s/mg ($n = 6$; standard deviation [SD] = 0.069), while *cydAB* membranes respired at a rate of 1.2 nmol/s/mg ($n = 4$; SD = 0.023). The result for the wild type is similar to the value of 3.8 (±0.16) nmol/s/mg calculated (18) for respiration of wild-type membranes, also using 5 mM formate as the electron donor. Oxygen uptake by wild-type (Fig. 6A) and *cydAB* membranes (Fig. 6B) typically reached a plateau at approximately 15% (33 μM) oxygen saturation and was unsuitable for oxygen affinity measurements. The inset in Fig. 6A shows the partial deoxygenation of oxyleghemoglobin. We considered the possibility that the failure to deoxygenate fully aerated buffer in the oxygen electrode was a result of the loss of soluble components required for electron transfer from formate to O_2. Indeed, membranes prepared from glucose-grown *E. coli* are incapable of catalyzing ATP- and succinate-driven NAD^+ reduction unless soluble fractions from broken cells are added, revealing the loss of dehydrogenases (36). Therefore, a portion of fresh cytoplasmic fraction (200 μl) was added to the electrode chamber before the addition of formate, as shown by arrows a in Fig. 6C and D. No stimulation of respiratory activity was observed.

Ligand-binding reactions of the terminal oxidases in *C. jejuni* studied using low-temperature photodissociation spectrophotometry. To record such spectra, cells were reduced, incubated with CO, transferred to the cryogenic apparatus of a dual-wavelength spectrophotometer, and photolyzed in situ. Figure 7 (top spectrum, dashed line) shows, for reference purposes, an inverted CO difference [i.e., reduced minus (reduced plus CO)] spectrum for wild-type *C. jejuni* cells, which would

TABLE 2. Oxygen affinities of *C. jejuni* wild-type and *cydAB* whole cells measured from the deoxygenation kinetics of oxyleghemoglobin and oxymyoglobin

Strain	Leghemoglobin[a]			Myoglobin[a]		
	K_m (nM)		V_{max} (nmol/mg/s)[b]	K_m (μM)		V_{max} (nmol/mg/s)[b]
	Lineweaver-Burk	Eadie-Hofstee		Lineweaver-Burk	Eadie-Hofstee	
Wild type	41 (3.9)	40 (0)	6.25 (2.5)	0.81 (0.015)	0.85 (0.056)	20[c]
cydAB mutant (Cio$^-$)	44 (6.4)	40 (8.2)	9.25 (0.96)	—[d]	—[d]	—[d]

[a] All values are means of four determinations, with standard deviations shown in parentheses.
[b] Calculated from Lineweaver-Burk plots or plots of *V* against *S*.
[c] One determination, but values in the range of 20 to 36 nmol/mg/s were measured with different batches of cells and myoglobin.
[d] —, no component detected

be expected to resemble the photodissociation spectrum. However, the attempted photodissociation spectrum recorded using wild-type whole cells at −120°C (Fig. 7A, lower trace) shows only a minor peak at 403 nm, with troughs at 417 and 551.5 nm. It is likely that *b*- and *c*-type hemes are responsible for these features, but the redox and ligation states are unclear. The most striking and puzzling feature of these spectra is the absence of any peak in the Soret region, corresponding to unligated ferrous heme, at approximately 430 nm, unlike the spectra recorded for cytochrome *cb′* oxidase-containing *Bradyrhizobium japonicum* (51). The 403-nm signal is also present in cytoplasmic fractions from wild-type cells (data not shown) and therefore may be due to a *c*-type heme capable of interaction with CO, as in the cytochrome *c*-containing CcoP subunits of the cytochrome *cb′* oxidases of *B. japonicum* and *Pseudomonas stutzeri* (32). The trough at approximately 415 to 417 nm was observed in the photodissociation spectra recorded for wild-type membranes and cytoplasmic fractions (not shown) and may represent both *b*- and *c*-type cytochromes. The 417-nm position of the minima in anoxic photodissociation spectra of *C. jejuni* differs from the wavelength of 427 to 429 nm recorded for the presence of a trough in the anoxic photodissociation spectra of *B. japonicum* (51) attributed to cytochrome *cb′*. The visible regions in spectra recorded for wild-type membranes and cytoplasmic fractions of *C. jejuni* (not shown) show features near 552 nm, which are presumably due to *c*-type hemes. The photodissociation spectra obtained for *cydAB* whole cells, membranes, and soluble fractions were broadly similar to those observed in the case of wild-type *C. jejuni*, suggesting that the "cytochrome *bd*-like oxidase" was not a major contributor to the overall photodissociation signals. No temperature-dependent CO recombination was observed over the range of −60 to −120°C (data not shown). In conclusion, photodissociation spectroscopy showed features of neither a *bd*-type oxidase nor an oxidase whose CO complex could be photodissociated to give an observable reduced species within the scan times employed here.

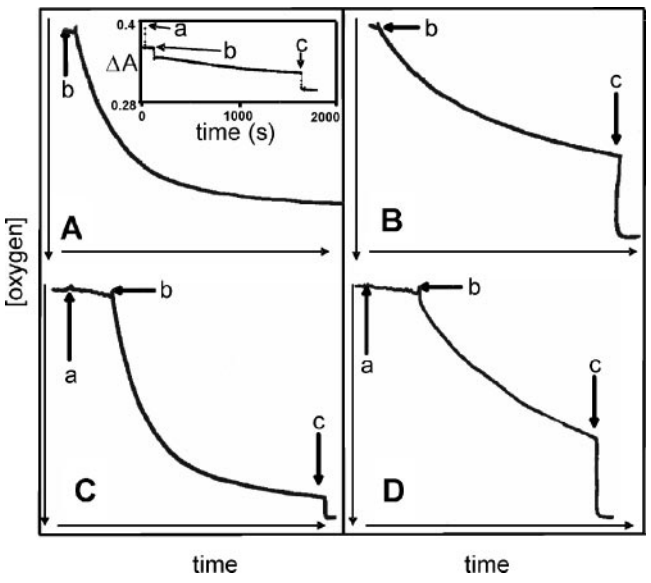

FIG. 6. Formate-supported respiration by membranes from wild-type and *cydAB* cells grown in liquid batch culture at 10% oxygen. Measurements were made with an oxygen electrode (A to D) or by following the partial deoxygenation of oxyleghemoglobin (inset in panel A). Panels A and C show oxygen consumption by membranes from wild-type cells. For panels A to D, 5 mM formate was added to stimulate the uptake of oxygen at time b, and dithionite was added at time c. In each, the vertical [oxygen] bar represents 220 μM, and the horizontal time bar represents 34, 27, 33, and 27 min (panels A, B, C, and D, respectively). For panels C and D only, 200 μl of the soluble fraction was added at time a (ω = 0.18 mg and 0.36 mg, respectively). For the inset, at time zero, the cuvette contained oxyleghemoglobin (17 μM) in buffer previously sparged with nitrogen. Formate (5 mM) was added at time a, membranes (ω = 0.53 mg) were added at time b, and sodium dithionite was added at time c.

Carbon monoxide reduction in *C. jejuni*? The spectroscopic data in Fig. 7 might be explained by the cytochrome *cb′* oxidase of *C. jejuni* having CO reductase activity, as spectra for both wild-type and *cydAB* strains recorded after photolysis appear to be in an oxidized rather than reduced state. Indeed, an oxidized-minus-(reduced plus CO) spectrum superimposed over the photodissociation spectrum of wild-type whole cells (Fig. 7B) reveals similarities between the oxidized and photodissociated states. This suggests that the cytochrome *cb′* oxidase possesses photolysis-dependent CO reductase activity that results in oxidation of redox proteins. Unusual CO reductase activity by which CO is converted to formaldehyde has been observed in the *bb′* oxidase of *Pseudomonas nautica* (2), in a reaction that is dependent on photolysis. To determine whether the cytochrome *bb′* oxidase of *C. jejuni* is capable of catalyzing CO reduction, formaldehyde, presumed to be generated by oxidase-mediated CO reduction, was assayed in whole cells and membranes of *C. jejuni*, but no significant levels were detectable in any fraction.

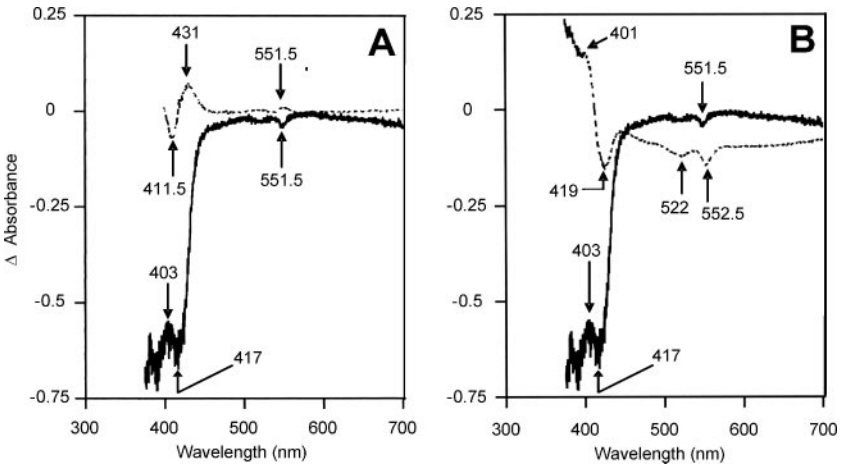

FIG. 7. Low-temperature photodissociation spectroscopy of reduced, CO-ligated *C. jejuni* cells. Panel A shows a comparison of a typical photodissociation spectrum (photolyzed minus CO-ligated spectrum, −120°C) (bottom) and the inverted CO difference spectrum (reduced minus CO-ligated spectrum, 22°C) (top). Cell concentrations were 5 and 3 mg/ml, respectively. Panel B compares the photodissociation spectrum (bold, continuous line) and an oxidized minus CO-ligated difference spectrum (dashed line), both at −120°C and 5 mg/ml. All spectra were recorded in dual-wavelength mode, using a 500-nm reference wavelength.

DISCUSSION

This paper reports the most detailed studies to date of respiratory oxidases in *C. jejuni*. The *cydAB*-encoded oxidase is not essential for growth under any condition tested, despite *cydAB* and *cydDC* mutants of *E. coli* and other bacteria being hypersensitive to zinc ions, cyanide, Fe(III) chelators, and protonophores (35). However, the *C. jejuni cydAB*-encoded oxidase improves the survival of *C. jejuni* under microaerobic conditions (Fig. 1). The atypical response of *C. jejuni* to stationary phase, in which cell viability declines precipitously, has been reported before (22). Reduced capacities for growth and stationary-phase survival have also been observed for *cydAB* mutants of other bacteria, including *E. coli* (44) and *Azotobacter vinelandii* (13). The *c*- and *b*-type cytochromes (18, 24) are not significantly different in wild-type and *cydAB* strains, but no features attributable to components of the presumed cytochrome *bd*-type oxidase were detected, whether assayed by (i) reduced-minus-oxidized room-temperature difference spectroscopy, (ii) CO difference spectroscopy, or (iii) CO photodissociation spectroscopy at subzero temperatures. Thus, the high-spin hemes *d* and b_{595} characteristic of cytochromes *bd* are absent from *C. jejuni*. Interestingly, the *cioAB* genes of *Pseudomonas aeruginosa* also encode peptides homologous to the two subunits of bacterial cytochromes *bd*, but here too, the cells do not display characteristic cytochrome *bd* features (7). Therefore, the CydAB-type terminal oxidase of *C. jejuni* (31) should be renamed CioAB, in deference to the *P. aeruginosa* example, the first oxidase shown (6) to be encoded by *cydAB*-like genes yet lacking the characteristic signals of cytochromes b_{558}, b_{595}, and *d*. It seems likely that the *cioAB*-encoded oxidases of *P. aeruginosa* and *C. jejuni* belong to the same family of poorly characterized enzymes in which the three hemes of classical cytochrome *bd*, i.e., hemes b_{558}, b_{595}, and *d*, are replaced by other (as yet unknown) redox centers. It is known that oxidases can display promiscuity with respect to the type of heme incorporated at the active site (40).

The operation of cyanide-sensitive and cyanide-insensitive systems in campylobacters was reported earlier (24). Typical cytochrome *bd*-type oxidases confer resistance to cyanide, including those of *E. coli* (41) and *A. vinelandii* (19). However, cyanide resistance does not necessarily require the presence of cytochrome *d* (1). Indeed, the KCN-insensitive oxidase of the respiratory chain of *P. aeruginosa* does not contain cytochrome *d* (6), yet membranes prepared from a *cio* mutant strain exhibit lowered oxygen consumption rates compared to those from the wild type in the presence of 1 mM KCN (7), and a *cio* mutant exhibits a MIC for KCN that is two- to fourfold lower than that for the wild-type strain (55). Cytochrome *cb′* oxidases are typically more sensitive to the inhibitory effects of cyanide than are CydAB-type oxidases (e.g., see reference 28).

In view of the microaerophilic lifestyle of *C. jejuni*, the oxygen reactivities of the oxidases are of special interest. Earlier studies of formate oxidation by *C. sputorum* subsp. *bubulus* identified two components with K_m values of 4 μM and 1 mM (30). However, the oxygen electrode used would be incapable of revealing high-affinity oxidases such as the *ccoNOQP*-encoded oxidase (31), believed to be of the cytochrome *cb′* type (cbb_3). Such oxidases were first identified in *Bradyrhizobium japonicum* (38) and subsequently found in pathogenic bacteria, including *Helicobacter pylori* (28). It is frequently stated that cytochrome *cb′* oxidases appear to perform a specialized role in bacterial microaerobic respiration (32), but only a few previous studies have described measurements made with an appropriately sensitive method, although the related FixNOQP oxidase of *B. japonicum* has been assigned an extremely low K_m value of 7 nM (39) by globin deoxygenation methods. The present leghemoglobin analyses suggest that the V_{max} for the respiratory chain in wild-type cells is lower than the V_{max} for *cioAB* mutant cells when expressed per mg of cell protein. This apparently surprising result may have several explanations. First, mutation of *cioAB* may result in up-regulation of synthesis of the high-affinity oxidase, which is not readily detectable in the complex CO spectra. Second, mutation of the cyanide-insensitive oxidase might divert electron flow to the high-af-

finity oxidase, supporting higher electron flux rates, particularly at the low oxygen tensions employed in these experiments.

In terms of its oxygen reactivity, *C. jejuni* CioAB resembles the *cydAB*-encoded oxidase of *Azotobacter vinelandii* (K_m value of 4.5 to 5.7 μM) (9) rather than the high-affinity cytochrome *bd* of *E. coli* (K_m, 4.5 nM) (8). It is tempting to speculate that *C. jejuni* CioAB has a special role in oxygen detoxification, as proposed for *A. vinelandii* CydAB, where cytochrome *bd* protects the oxygen-labile nitrogenase, allowing aerotolerant nitrogen fixation (23). In the case of *C. jejuni*, the role of CioAB may be in lowering oxygen levels and maintaining microaerobic conditions.

The possession of two or more terminal oxidases with different properties (such as oxygen affinity and inhibitor resistance, as exemplified by *C. jejuni*) is a common theme in bacterial physiology (35). In this study, *cioAB* expression was shown to increase fivefold under O_2-replete laboratory conditions, consistent with the lower O_2 affinity of the oxidase and the increased cyanide resistance of cultures grown under these conditions. The relative importance of the two oxidases in *C. jejuni* physiology in vivo is unclear, but two microarray studies are of interest in light of the oxygen affinities reported here. Transcriptional profiling of *C. jejuni* during colonization of the chick cecum showed that the *cco* genes—shown in the present study to encode the very-high-affinity oxidase—were up-regulated about fourfold (53), suggesting a microaerobic environmental niche. However, expression profiling to determine gene expression in *C. jejuni* recovered from rabbit ileal loops (compared with bacteria grown in vitro to mid-logarithmic phase) (47) showed that *cioAB* expression was elevated 350-fold in vivo compared to that in vitro. The authors concluded that the in vivo transcriptome is consistent with an oxygen-limited environment but assumed that the *C. jejuni* CydAB-type oxidase has a high affinity for oxygen, whereas our results clearly show that this oxidase has a low oxygen affinity in *C. jejuni*. Furthermore, elevated expression of *cydAB* in the ileal loop was accompanied by up-regulation of *fdh* genes, encoding formate dehydrogenase—which has been shown in the present work to support a robust oxygen-consuming activity—and by down-regulation of all genes encoding reductases involved in electron transfer to oxidants other than oxygen, i.e., fumarate, nitrate, nitrite, and N- or O-oxides (43). These microarray results suggest that there is an aerobic environment in ileal loops.

Despite the reported increase in *cioAB* expression in vivo (47), there is clear evidence that *cioAB* is also expressed in vitro. First, we report here that RT-PCR readily measures *cioAB* transcription and demonstrates increased transcription under oxygen-replete conditions. Second, in unpublished microarray profiling of *C. jejuni* cells grown in vitro (C. E. Monk and R. K. Poole, unpublished data), the *cioAB* transcripts were detectable, with spot intensities (after background correction) on the same order as, for example, the transcripts of *ctb*, encoding the truncated hemoglobin of *C. jejuni*, and with intensities greater than the transcripts of *cgb*, encoding the NO-detoxifying hemoglobin, under noninducing conditions (49). The spectroscopic invisibility of the oxidase in comparison of the wild-type and mutant strains (Fig. 2) does not preclude a functional role for CioAB in O_2 consumption. Consider the situation where CioAB makes only a 5% contribution to the CO difference spectrum in Fig. 2B and is therefore regarded as undetectable. The absorption coefficient for this oxidase is unknown, but if we assume a value of 91 mM^{-1} cm^{-1}, as for mitochondrial cytochrome *c* oxidase (cytochrome a_3) (4), the concentration of oxidase represented by the CO difference spectrum is 0.08 nmol/ml or 0.027 nmol/mg protein. The total respiration rate of intact cells is on the order of 15 nmol oxygen consumed/mg protein/s (Tables 1 and 2), and assuming the operation of only the CioAB-type oxidase, it would require a turnover number of 550 s^{-1}. An established literature value for the turnover number of the mitochondrial oxidase (both for the isolated enzyme and in situ) is 400 s^{-1} (50). That is, an oxidase with typical spectroscopic and kinetic properties that contributes only 5% to the visible spectrum could account for >70% of measured respiration rates.

The CO difference spectra (Fig. 2B) show a strong absorbance minimum at 431 nm, which is similar to the trough assigned to cytochrome *o* in *E. coli* (37), but the 411.5-nm peak is considerably shifted toward blue from the position expected. Furthermore, signals in the α/β regions of Fig. 2B are indicative of low-spin CO-binding species (52), not cytochrome *o* (37). However, the most persuasive evidence for the lack of cytochrome *o*-like ligand-binding behavior comes from the anoxic photodissociation spectrum, in which all the characteristic features of the cytochrome *o* spectrum are lacking (Fig. 7). The ligand-binding and possibly CO-reductive properties of the terminal oxidases of *C. jejuni* require further investigation, particularly given the finding that the primary structures of the major subunits of the "cbb_3 type" indicate that they belong to a separate group within the cytochrome cbb_3 family (45).

In conclusion, we have identified two terminal oxidases with significantly different catalytic capabilities in the aerobic respiratory chain of *C. jejuni*. The cyanide-insensitive CioAB-type oxidase, the product of the so-called *cydAB* genes, is of low O_2 affinity (K_m = 0.8 μM). It is dispensable for microaerobic growth and respiration but required for optimal microaerobic survival, and gene expression is increased at higher O_2 provision rates. In contrast to earlier assumptions (45), we found no evidence that this oxidase is of the cytochrome *bd* type. The cytochrome *cb′* oxidase has a typical high affinity for oxygen, displaying a K_m value of 40 nM. This cyanide-sensitive oxidase may act as the dominant oxidase for the microaerobic growth of *C. jejuni*, since we were unable to construct a mutant deficient in cytochrome *cb′*. The reactions of the atypical CioAB-type oxidase of *C. jejuni* with ligands and its possible CO reductase activity also require further study.

ACKNOWLEDGMENTS

This study was supported by BBSRC grants D18084 and BFP11346 to R.K.P. and S.F.P. and by a BBSRC studentship to R.J.J.

We are grateful to Colin Jones, Julian Ketley, Jo Cox (all from University of Leicester), and Claire Monk (The University of Sheffield) for communicating unpublished results, Huw Williams (Imperial College) for valuable discussions and the CioA antibody, Mark Johnson for technical support, David Kelly (The University of Sheffield) for useful suggestions, Arthur Moir and Julie Scholes (The University of Sheffield) for peptide synthesis and RT-PCR access, respectively, and F. J. Bergersen (CSIRO, Canberra, Australia) for the gift of leghemoglobin.

REFERENCES

1. **Akimenko, V. K., and S. M. Trutko.** 1984. On the absence of correlation between cyanide-resistant respiration and cytochrome *d* content in bacteria. Arch. Microbiol. **138:**58–63.

1a. **Applied Biosystems.** User bulletin 2. ABI Prism 7700 sequence detection system: relative quantification of gene expression. Applied Biosystems, Foster City, CA.

2. **Arnaud, S., F. Malatesta, and M. Denis.** 1992. Reduction of carbon monoxide to formaldehyde by the terminal oxidase of the marine bacterium *Pseudomonas nautica* strain-617. FEBS Lett. **296:**259–262.

3. **Bergersen, F. J., and G. L. Turner.** 1979. Systems utilizing oxygenated leghemoglobin and myoglobin as sources of free dissolved O_2 at low concentrations for experiments with bacteria. Anal. Biochem. **96:**165–174.

4. **Chance, B.** 1957. Techniques for the assay of the respiratory enzymes. Methods Enzymol. **4:**273–329.

5. **Cooper, M., G. R. Tavankar, and H. D. Williams.** 2003. Regulation of expression of the cyanide-insensitive terminal oxidase in *Pseudomonas aeruginosa*. Microbiology **149:**1275–1284.

6. **Cunningham, L., M. Pitt, and H. D. Williams.** 1997. The *cioAB* genes from *Pseudomonas aeruginosa* code for a novel cyanide-insensitive terminal oxidase related to the cytochrome *bd* quinol oxidases. Mol. Microbiol. **24:**579–591.

7. **Cunningham, L., and H. D. Williams.** 1995. Isolation and characterization of mutants defective in the cyanide-insensitive respiratory pathway of *Pseudomonas aeruginosa*. J. Bacteriol. **177:**432–438.

8. **D'mello, R., S. Hill, and R. K. Poole.** 1996. The cytochrome *bd* quinol oxidase in *Escherichia coli* has an extremely high oxygen affinity and two oxygen-binding haems: implications for regulation of activity *in vivo* by oxygen inhibition. Microbiology **142:**755–763.

9. **D'mello, R., S. Hill, and R. K. Poole.** 1994. Determination of the oxygen affinities of terminal oxidases in *Azotobacter vinelandii* using the deoxygenation of oxyleghaemoglobin and oxymyoglobin: cytochrome *bd* is a low-affinity oxidase. Microbiology **140:**1395–1402.

10. **D'mello, R., S. Hill, and R. K. Poole.** 1995. The oxygen affinity of cytochrome *bo′* in *Escherichia coli* determined by the deoxygenation of oxyleghemoglobin and oxymyoglobin: K_m values for oxygen are in the submicromolar range. J. Bacteriol. **177:**867–870.

11. **Dowd, J. E., and D. S. Riggs.** 1965. A comparison of estimates of Michaelis-Menten kinetic constants from various linear transformations. J. Biol. Chem. **240:**863–869.

12. **Dueweke, T. J., and R. B. Gennis.** 1990. Epitopes of monoclonal antibodies which inhibit ubiquinol oxidase activity of *Escherichia coli* cytochrome *d* complex localize functional domain. J. Biol. Chem. **265:**4273–4277.

13. **Edwards, S. E., C. S. Loder, G. Wu, H. Corker, B. W. Bainbridge, S. Hill, and R. K. Poole.** 2000. Mutation of cytochrome *bd* quinol oxidase results in reduced stationary phase survival, iron deprivation, metal toxicity and oxidative stress in *Azotobacter vinelandii*. FEMS Microbiol. Lett. **185:**71–77.

14. **Elvers, K. T., S. M. Turner, L. M. Wainwright, G. Marsden, J. Hinds, J. A. Cole, R. K. Poole, C. W. Penn, and S. F. Park.** 2005. NssR, a member of the Crp-Fnr superfamily from *Campylobacter jejuni*, regulates a nitrosative stress-responsive regulon that includes both a single-domain and a truncated haemoglobin. Mol. Microbiol. **57:**735–750.

15. **Friedman, C. R., J. Neimann, H. C. Wegener, and R. V. Tauxe.** 2000. Epidemiology of *Campylobacter jejuni* infections in the United States and other industrialized nations, p. 121–138. *In* I. Nachamkin and M. J. Blaser (ed.), *Campylobacter*, 2nd ed. ASM Press, Washington, DC.

16. **Goodhew, C. F., A. B. Elkurdi, and G. W. Pettigrew.** 1988. The microaerophilic respiration of *Campylobacter mucosalis*. Biochim. Biophys. Acta **933:**114–123.

17. **Hickey, T. E., A. L. McVeigh, D. A. Scott, R. E. Michielutti, A. Bixby, S. A. Carroll, A. L. Bourgeois, and P. Guerry.** 2000. *Campylobacter jejuni* cytolethal distending toxin mediates release of interleukin-8 from intestinal epithelial cells. Infect. Immun. **68:**6535–6541.

18. **Hoffman, P. S., and T. G. Goodman.** 1982. Respiratory physiology and energy conservation efficiency of *Campylobacter jejuni*. J. Bacteriol. **150:**319–326.

19. **Jones, C. W.** 1973. The inhibition of *Azotobacter vinelandii* terminal oxidases by cyanide. FEBS Lett. **36:**347–350.

20. **Jones, C. W., and E. R. Redfearn.** 1966. Electron transport in *Azotobacter vinelandii*. Biochim. Biophys. Acta **113:**467–481.

21. **Kalnenieks, U., N. Galinina, S. Bringer-Meyer, and R. K. Poole.** 1998. Membrane D-lactate oxidase in *Zymomonas mobilis*: evidence for a branched respiratory chain. FEMS Microbiol. Lett. **168:**91–97.

22. **Kelly, A. F., S. F. Park, R. Bovill, and B. M. Mackey.** 2001. Survival of *Campylobacter jejuni* during stationary phase: evidence for the absence of a phenotypic stationary-phase response. Appl. Environ. Microbiol. **67:**2248–2254.

23. **Kelly, M. J. S., R. K. Poole, M. G. Yates, and C. Kennedy.** 1990. Cloning and mutagenesis of genes encoding the cytochrome *bd* terminal oxidase complex in *Azotobacter vinelandii*: mutants deficient in the cytochrome *d* complex are unable to fix nitrogen in air. J. Bacteriol. **172:**6010–6019.

24. **Lascelles, J., and K. M. Calder.** 1985. Participation of cytochromes in some oxidation-reduction systems in *Campylobacter fetus*. J. Bacteriol. **164:**401–409.

25. **Markwell, M. A. K., S. M. Haas, L. L. Bieber, and N. E. Tolbert.** 1978. A modification of the Lowry procedure to simplify protein determination in membrane and lipoprotein samples. Anal. Biochem. **87:**206–210.

26. **Moss, C. W., M. A. Lambert-Fair, M. A. Nicholson, and G. O. Guerrant.** 1990. Isoprenoid quinones of *Campylobacter cryaerophila*, *C. cinaedi*, *C. fennelliae*, *C. hyointestinalis*, *C. pylori*, and "*C. upsaliensis*". J. Clin. Microbiol. **28:**395–397.

27. **Nachamkin, I.** 2002. Chronic effects of *Campylobacter* infection. Microbes Infect. **4:**399–403.

28. **Nagata, K., S. Tsukita, T. Tamura, and N. Sone.** 1996. A *cb*-type cytochrome-*c* oxidase terminates the respiratory chain in *Helicobacter pylori*. Microbiology **142:**1757–1763.

29. **Niekus, H. G. D., E. van Doorn, W. de Vries, and A. H. Stouthamer.** 1980. Aerobic growth of *Campylobacter sputorum* subspecies *bubulus* with formate. J. Gen. Microbiol. **118:**419–428.

30. **Niekus, H. G. D., E. van Doorn, and A. H. Stouthamer.** 1980. Oxygen consumption by *Campylobacter sputorum* subspecies *bubulus* with formate as substrate. Arch. Microbiol. **127:**137–143.

31. **Parkhill, J., B. W. Wren, K. Mungall, J. M. Ketley, C. Churcher, D. Basham, T. Chillingworth, R. M. Davies, T. Feltwell, S. Holroyd, K. Jagels, A. V. Karlyshev, S. Moule, M. J. Pallen, C. W. Penn, M. A. Quail, M. A. Rajandream, K. M. Rutherford, A. H. M. vanVliet, S. Whitehead, and B. G. Barrell.** 2000. The genome sequence of the food-borne pathogen *Campylobacter jejuni* reveals hypervariable sequences. Nature **403:**665–668.

32. **Pitcher, R. S., M. R. Cheesman, and N. J. Watmough.** 2002. Molecular and spectroscopic analysis of the cytochrome *cbb*(3) oxidase from *Pseudomonas stutzeri*. J. Biol. Chem. **277:**31474–31483.

33. **Poole, R. K.** 1977. The influence of growth substrate and capacity for oxidative phosphorylation on respiratory oscillations in synchronous cultures of *Escherichia coli* K12. J. Gen. Microbiol. **99:**369–377.

34. **Poole, R. K.** 1993. The isolation of membranes from bacteria. Methods Mol. Biol. **19:**109–122.

35. **Poole, R. K., and G. M. Cook.** 2000. Redundancy of aerobic respiratory chains in bacteria? Routes, reasons and regulation. Adv. Microb. Physiol. **43:**165–224.

36. **Poole, R. K., and B. A. Haddock.** 1974. Energy-linked reduction of nicotinamide-adenine dinucleotide in membranes derived from normal and various respiratory-deficient mutant strains of *Escherichia coli* K12. Biochem. J. **144:**77–85.

37. **Poole, R. K., A. J. Waring, and B. Chance.** 1979. The reaction of cytochrome *o* in *Escherichia coli* with oxygen. Low-temperature kinetic and spectral studies. Biochem. J. **184:**379–389.

38. **Preisig, O., D. Anthamatten, and H. Hennecke.** 1993. Genes for a microaerobically induced oxidase complex in *Bradyrhizobium japonicum* are essential for a nitrogen-fixing endosymbiosis. Proc. Natl. Acad. Sci. USA **90:**3309–3313.

39. **Preisig, O., R. Zufferey, L. Thonymeyer, C. A. Appleby, and H. Hennecke.** 1996. A high-affinity cbb_3-type cytochrome oxidase terminates the symbiosis-specific respiratory chain of *Bradyrhizobium japonicum*. J. Bacteriol. **178:**1532–1538.

40. **Puustinen, A., J. E. Morgan, M. Verkhovsky, J. W. Thomas, R. B. Gennis, and M. Wikstrom.** 1992. The low-spin heme site of cytochrome *o* from *Escherichia coli* is promiscuous with respect to heme type. Biochemistry **31:**10363–10369.

41. **Rice, C. W., and W. P. Hempfling.** 1978. Oxygen-limited continuous culture and respiratory energy conservation in *Escherichia coli*. J. Bacteriol. **134:**115–124.

42. **Rozen, S., and H. J. Skaletsky.** 2000. Primer3 on the WWW for general users and for biologist programmers. Methods Mol. Biol. **132:**365–386.

43. **Sellars, M. J., S. J. Hall, and D. J. Kelly.** 2002. Growth of *Campylobacter jejuni* supported by respiration of fumarate, nitrate, nitrite, trimethylamine-*N*-oxide, or dimethyl sulfoxide requires oxygen. J. Bacteriol. **184:**4187–4196.

44. **Siegele, D. A., K. R. Imlay, and J. A. Imlay.** 1996. The stationary-phase-exit defect of *cydC* (*surB*) mutants is due to the lack of a functional terminal cytochrome oxidase. J. Bacteriol. **178:**6091–6096.

45. **Smith, M. A., M. Finel, V. Korolik, and G. L. Mendz.** 2000. Characteristics of the aerobic respiratory chains of the microaerophiles *Campylobacter jejuni* and *Helicobacter pylori*. Arch. Microbiol. **174:**1–10.

46. **Stevanin, T. M., N. Ioannidis, C. E. Mills, S. O. Kim, M. N. Hughes, and R. K. Poole.** 2000. Flavohemoglobin Hmp affords inducible protection for *Escherichia coli* respiration, catalyzed by cytochromes *bo′* or *bd*, from nitric oxide. J. Biol. Chem. **275:**35868–35875.

47. **Stintzi, A., D. Marlow, K. Palyada, H. Naikare, R. Panciera, L. Whitworth, and C. Clarke.** 2005. Use of genome-wide expression profiling and mutagenesis to study the intestinal lifestyle of *Campylobacter jejuni*. Infect. Immun. **73:**1797–1810.

48. **van Vliet, A. H. M., K. G. Wooldridge, and J. M. Ketley.** 1998. Iron-responsive gene regulation in a *Campylobacter jejuni fur* mutant. J. Bacteriol. **180:** 5291–5298.
49. **Wainwright, L. M., K. T. Elvers, S. F. Park, and R. K. Poole.** 2005. A truncated haemoglobin implicated in oxygen metabolism by the microaerophilic food-borne pathogen *Campylobacter jejuni*. Microbiology **151:**4079–4091.
50. **Wikstrom, M., K. Krab, and M. Saraste.** 1981. Cytochrome oxidase. A synthesis. Academic Press, London, United Kingdom.
51. **Williams, H. D., C. A. Appleby, and R. K. Poole.** 1990. The unusual behaviour of the putative terminal oxidases of *Bradyrhizobium japonicum* bacteroids revealed by low-temperature photodissociation studies. Biochim. Biophys. Acta **1019:**225–232.
52. **Wood, P. M.** 1984. Bacterial proteins with CO-binding b- or c-type haem. Functions and absorption spectroscopy. Biochim. Biophys. Acta **768:**293–317.
53. **Woodall, C. A., M. A. Jones, P. A. Barrow, J. Hinds, G. L. Marsden, D. J. Kelly, N. Dorrell, B. W. Wren, and D. J. Maskell.** 2005. *Campylobacter jejuni* gene expression in the chick cecum: evidence for adaptation to a low-oxygen environment. Infect. Immun. **73:**5278–5285.
54. **Wren, B. W., I. Henderson, and J. M. Ketley.** 1994. A PCR-based strategy for the rapid construction of defined bacterial deletion mutants. BioTechniques **16:**994–996.
55. **Zlosnik, J. E. A., G. R. Tavankar, J. G. Bundy, D. Mossialos, R. O'Toole, and H. D. Williams.** 2006. Investigation of the physiological relationship between the cyanide-sensitive oxidase and cyanide production in *Pseudomonas aeruginosa*. Microbiology **152:**1407–1415.